CONF-780611--10

PNL-SA-6721

A Model for Predicting Dry Deposition of Particles and Gases to Environmental Surfaces

by
G. A. Sehmel
W. H. Hodgson

January 1978

Prepared for the
U.S. Department of Energy
under Contract EY-76-C-06-1830

MASTER

Battelle
Pacific Northwest Laboratories

PNL-SA-6721

DISTRIBUTION OF THIS DOCUMENT IS UNLIMITED

DISCLAIMER

This report was prepared as an account of work sponsored by an agency of the United States Government. Neither the United States Government nor any agency Thereof, nor any of their employees, makes any warranty, express or implied, or assumes any legal liability or responsibility for the accuracy, completeness, or usefulness of any information, apparatus, product, or process disclosed, or represents that its use would not infringe privately owned rights. Reference herein to any specific commercial product, process, or service by trade name, trademark, manufacturer, or otherwise does not necessarily constitute or imply its endorsement, recommendation, or favoring by the United States Government or any agency thereof. The views and opinions of authors expressed herein do not necessarily state or reflect those of the United States Government or any agency thereof.

DISCLAIMER

Portions of this document may be illegible in electronic image products. Images are produced from the best available original document.

PNL-SA-6721

A MODEL FOR PREDICTING DRY DEPOSITION OF PARTICLES AND GASES TO ENVIRONMENTAL SURFACES

Prepared for presentation at the 85th American Institute of Chemical Engineers National meeting, June 4-8, 1978, Philadelphia, Pennsylvania

by
G. A. Sehmel and W. H. Hodgson

This work was done for the Department of Energy under Contract EY-76-C-06-1830 with Battelle, Pacific Northwest Laboratory

The submitted manuscript has been authorized by a contractor of the U.S. Government under Contract EY-76-C-06-1830. Accordingly, the U.S. Government retains a nonexclusive, royalty-free license to publish or reproduce the published form of this contribution, or allow others to do so, for U.S. Government purposes.

January 1978

NOTICE
This report was prepared as an account of work sponsored by the United States Government. Neither the United States nor the United States Department of Energy, nor any of their employees, nor any of their contractors, subcontractors, or their employees, makes any warranty, express or implied, or assumes any legal liability or responsibility for the accuracy, completeness or usefulness of any information, apparatus, product or process disclosed, or represents that its use would not infringe privately owned rights.

BATTELLE
PACIFIC NORTHWEST LABORATORIES
RICHLAND, WA 99352

CONTENTS

ABSTRACT 1

INTRODUCTION. 1

GENERAL MODEL 5

SIMPLE MODEL 6

Int_3 9

Int_2 and Int_1 11

Integral Resistance Ranges. 11

Deposition Velocity as a Function of Height 13

Controlling Mass Transfer Resistances 15

Deposition Velocity as a Function of Friction Velocity 17

Deposition Velocities at 1 m 20

CANOPY LIMITATION 29

CONCLUSIONS 35

ACKNOWLEDGMENT 37

NOMENCLATURE 37

APPENDIX 39

Roughness Height and Friction Velocity. 39

REFERENCES 41

FIGURES

1. Resistance Integral from 1 cm to Indicated Height 12

2. Model-1977W - Predicted Deposition Velocities at Indicated Height for U_* = 20.0 cm/sec, Z_o = 3.0 cm and Particle Density = 1.0 g/cm^3 14

3. Model-1977W - Predicted Deposition Velocities at Indicated Height for U_* = 20 cm/sec, Z_o = 3.0 cm with no Surface Resistance (INT_3=0) Below 1 cm and Particle Density = 1.0 g cm^3 16

4. Model-1977W - Predicted Deposition Velocities at 1M Height for Z_o = 3.0 cm with no Ground Resistance (INT_3=0) Below 1 cm and Particle Density = 1.0 g/cm^3. 18

5. Model-1977W - Predicted Deposition Velocities at 1M Height for Z_o = 3.0 cm and Neutral $\varepsilon = kU_*Z$. 19

6. Model-1977W - Predicted Deposition Velocities at 1M for U_* = 30 cm/sec and Particle Densities of 1, 4 and 11.5 g cm^3. 21

7. Model-1977W - Predicted Deposition Velocities at 1M for U_* = 10 cm/sec and Particle Densities of 1, 4 and 11.5 g/cm^3. 22

8. Model-1977W - Predicted Deposition Velocities at 1M for U_* = 20 cm/sec and Particle Densities of 1, 4 and 11.5 g/cm^3. 23

9. Model-1977W - Predicted Deposition Velocities at IM, for U_* = 50 cm/sec and Particle Densities of 1, 4 and 11.5 g/cm^3. 24

10. Model-1977W - Predicted Deposition Velocities at 1M for U_* = 100 cm/sec and Particle Densities of 1, 4 and 11.5 g/cm^3. 25

11. Model-1977W - Predicted Deposition Velocities at 1M for U_* = 150 cm/sec and Particle Densities of 1, 4 and 11.5 g/cm^3. 26

12. Model-1977W - Predicted Deposition Velocities at 1M for U_* = 200 cm/sec and Particle Densities of 1, 4 and 11.5 g cm^3. 27

13. Deposition Velocities to a Canopy of Plastic Trees 9 cm High 30

14. Penetration of Depositing Particles Through a Canopy of Plastic Trees 31

15. Penetration of Depositing Particles Through 3.8 to 5.1 cm Diameter Crushed Rock to an Underlying Surface 32

TABLES

1. Experimental Range of Variables Used in Developing Integral Resistance Correlation. 9

A MODEL FOR PREDICTING DRY DEPOSITION OF PARTICLES AND GASES TO ENVIRONMENTAL SURFACES

G. A. Sehmel and W. H. Hodgson

Pacific Northwest Laboratory
Operated by Battelle Memorial Institute
Richland, Washington 99352

ABSTRACT

A predictive model is demonstrated for correlating particle and gas removal rates from the atmosphere by dry deposition. Predicted deposition rates can vary over several orders of magnitude and are complex functions of pollutant, air, and surface variables. The validity of many published field deposition measurements is discussed in terms of these complexities.

INTRODUCTION

Particle deposition velocities describe mass transfer rates at the air-surface interface and are a function of many variables including surface, particle, and meteorological parameters. These removal rates are important in considerations of air pollution removal if environmentally permissible upper limits of air pollutant concentrations are not to be exceeded. Deposition velocities have been summarized for several authors (1). Unfortunately, many experimental deposition velocities have been determined with limited control of experimental conditions. Particle diameters have been inadequately known, and hence experimental results have usually been reported with insufficient information to generalize deposition velocities to other field conditions. These limited field deposition velocity measurements have never been correlated into any predictive model.

Particle and gaseous removal rates are nonsteady-state processes dependent upon the delivery capability of the upper atmosphere as well

as surface mass transfer resistance within the cm adjacent to the deposition surface. Historically, deposition velocities, v_d, have been defined as a deposition flux, N, divided by an airborne concentration, χ, for a polydispersed aersosol.

That is,

$$v_d = \frac{(-N)}{\chi} \tag{1}$$

which has units of length/time usually reported as cm/sec. Airborne concentrations have often been measured at 1 m above the deposition surface.

There is a fallacy in this deposition velocity concept. It is the exception rather than rule that nonsteady-state mass transfer can be adequately described by a single point concentration measurement. If mass transfer occurs, a profile of airborne concentration as a function of height must develop to act as the driving gradient for mass transfer in a diffusion-controlled process. This assumes, of course, that particle transport can be described by Fickian diffusion. In the nominal case of simple gravity settling the airborne concentration will be constant with height.

In mass transfer processes the airborne concentration at any point results from the capability of the atmosphere to deliver pollutant from regions of higher concentrations to regions of lower concentrations. Consequently, most field determined deposition velocities only approximate surface mass transfer removal rates for the particular airborne pollutant plume test conditions which occur above the reference concentration measurement height. To extrapolate those field deposition velocities to new situations requires similitude between pollutant plume shape, particle diameters, wind shear, etc.

This paper presents a generalized technique for predicting particle removal rates by dry deposition from any airborne plume. The technique is based upon wind tunnel derived deposition velocities for monodispersed particles. Although the present results are the best statistical fit of

these data, the deposition velocity predictions to be developed show the same general dependency on particle diameter, friction velocity, aerodynamic surface roughness, and particle density as has been previously reported (2-7). A required assumption inherent in applying the method is that one can completely describe pollutant plume concentrations as a function of time and space. Otherwise, the usual assumption of a deposition velocity applicable to a 1 m reference height will be required. Predicted deposition velocities are given for a pollutant concentration reference height of 1 m.

GENERAL MODEL

Pollutant motion in the atmosphere is described by a multi-dimensional, nonsteady-state continuity equation which, conceptually, can be separated into a multi-box deposition model as a function of height above the deposition surface. The upper-most box is box 1 and the box at the deposition surface is box n. Conceptually, box n could even describe the stomatal resistance of an individual leaf. In the model, mass transfer resistances are calculated to describe the particle flux through the boxes from the reference concentration height to the deposition surface. Mathematical requirements are that concentrations and fluxes are equal at the juncture of adjoining boxes. There should be at least three boxes describing the overall deposition process.

In box 1, airborne pollutant plume vertical movement is described by standard (1) meteorological diffusion equations. In this turbulent atmospheric layer, mass transfer processes are described by micrometeorological eddy diffusivities. In the overall deposition process, the plume approaches and interfaces with box 2. This idealized layer of box 2 is just above the vegetative canopy or surface elements in a region where atmospheric transfer processes are modified by the canopy or surfaces. This interface region can extend to all scales from small vegetation and trees, to scales as large as cities. Box 3 is at and within the deposition surface canopy.

Deposition velocities are calculated from integral diffusional resistances in each of the three boxes. Predictions must be limited to surface elements with small roughness heights since a diffusional resistance correlation exists (2) only for small surface roughness. Perhaps as additional data are obtained, further model generalization to both larger roughness heights and sub-boxes within box 3 will be predictable.

Model predictions of deposition velocities using boxes 1 and 3 will be for the simplest case--steady state one-dimensional flow from a uniform pollutant source. Extension of model concepts to other pollutant plumes

is limited only by the reader's requirements and ability to predict pollutant concentrations caused by diffusion and transport at significant elevations above environmental surfaces. If the user has a plume surface depletion model available to predict concentrations at the interface of boxes 2 and 3, the user will not need the proposed simple model. Rather, the user should directly use the mass transfer resistance integral for box 3 in that more complex model.

Most diffusion transport equations still use a deposition velocity rather than a mass transfer integral for a boundary condition. Consequently, a method for predicting deposition velocities, K_1, will be presented. The deposition velocity, K, is defined as

$$K_1 = \frac{(-N)}{C} \tag{2}$$

In this case, the concentration, C, is for monodispersed particles and is measured 1 cm above the deposition surface. The deposition velocity nomenclature K, rather than v_d, reflects that deposition velocities are a function of particle diameter. Predictions shown will be for K_{1-m} rather than K_1. The subscript 1-m indicates a reference pollutant concentration at a 1 m reference height.

SIMPLE MODEL

Deposition velocities, K, are based on the assumption particle deposition is described by a one-dimensional, steady-state continuity equation. Basic assumptions in this model are that particles diffuse at a constant flux from a uniform concentration of particles, that a relationship for particle eddy diffusivity can be determined, that the effect of gravity can be described by the terminal settling velocity, that particle agglomeration does not occur, and that particles are completely retained by the surface. Based upon these assumptions, the deposition flux to a surface is described by

$$N = -(\varepsilon + D)\frac{dC}{dz} - v_t C, \tag{3}$$

in which v_t is the absolute value of the terminal settling velocity.

The deposition velocity is predicted from a dimensionless integral form of Eq. (3):

$$-\int_{C_z}^{0} \frac{u_* \, dC}{N + v_t C} = \int_{z^+ \text{ at } C_z}^{r+} \frac{dz+}{\varepsilon/\nu + D/\nu} = \text{Int} \tag{4}$$

in which ε is the particle eddy diffusivity, D is the Brownian diffusivity, ν is the kinematic viscosity of air, u_* is the friction velocity, $z^+ = zu_*/\nu$ is the dimensionless distance above the surface, and v_t is the particle terminal settling velocity. Integration limits are that particle concentrations is C_z at a reference height of z cm and that particle concentration is zero at a dimensionless particle radius, r^+, from the deposition surface.

The integral involving diffusion is a resistance integral (a negative value) abbreviated as Int. Since Int contains the dimensionless eddy diffusivity, ε/ν and Brownian diffusivity, Int quantifies only diffusional resistance between the integration limits. The integral, Int, can be subdivided into

$$\text{Int} = \int_{z^+ \text{ at } C_z}^{z^+_{1-2}} \frac{dz^+}{\varepsilon/\nu + D/\nu} + \int_{z^+_{1-2}}^{z^+_{2-3}} \frac{dz^+}{\varepsilon/\nu + D/\nu} + \text{Int}_3 \tag{5}$$

where the first integral in Box 1 is Int_1 and the second integral in Box 2 is Int_2. The limit, z^+_{1-2}, is the height at which boxes 1 and 2 interface. Similarly, boxes 2 and 3 interface at z^+_{2-3}. These integrals will be evaluated after a relationship between deposition velocity and Int is shown.

The deposition velocity is obtained from an integrated form of Eq. (4) for the deposition flux, N,

$$N = \frac{v_t \, C_z \, \alpha}{1 - \alpha} \tag{6}$$

in which

$$\alpha = \exp\,(-v_t \; Int/u_*). \tag{7}$$

Now the deposition velocity is defined in terms of the reference concentration, C_z at z cm height,

$$K_z = \frac{(-N)}{C_z} \; . \tag{8}$$

Thus, the deposition velocity at height z is

$$K_z = \frac{v_t}{1 - (1/\alpha)} \; . \tag{9}$$

As shown by Eq. (9), the lower limit of predicted deposition velocities is v_t. The reason for this limit is that if the diffusional resistance were large (Int is a negative number), α would approach infinity and $1/\alpha$ would approach zero. However, as diffusional resistance became relatively less, the deposition velocity would become increasingly greater than the gravitational settling velocity.

From the above equation, Int is related to a simple resistance R by,

$$R = \frac{1}{K} = \frac{1 - \exp\left(\frac{v_t}{u_*} \; Int\right)}{v_t} \; . \tag{10}$$

$\underline{Int_3}$

Surface integral resistances, Int_3 were evaluated from wind tunnel (9) determined deposition velocities. Experimentally, deposition velocities, K_1, were determined for deposition of monodispersed particles onto five different surfaces. The ranges of monodispersed particle diameter, friction velocity, and aerodynamic surface roughness investigated are shown in Table 1. Particle density was 1.5 g/cm^3. In all cases, the reference concentration height for defining K_1 was 1 cm above the deposition surface. This corresponds to a box 3 resistance. Consequently, values of Int_3 were evaluated from the K_1's by using the expression

$$Int_3 = \frac{u_*}{v_t} \ln(1 - v_t/K_1) \ . \qquad (11)$$

TABLE 1. Experimental Range of Variables Used in Developing Integral Resistance Correlation

Deposition Surface		Range of Variables Used in Developing INT Correlation		
Type	Dimensions, cm	Particle Diameter, μm	Friction Velocity, u_*, cm/sec	Roughness Height, z_0, cm
Brass shim stock	"smooth"	0.03 to 28	11 to 73	0.004
Artificial grass	0.7 height	0.03 to 28	19 to 144	0.12 to 0.40
Gravel	0.5 to 1.6 "diameter"	0.03 to 26	22 to 133	0.13 to 0.18
Water	Wave Height to 2.5 cm	0.03 to 29	11 to 122	0.001 to 0.002
Gravel	3.8 to 5.1 "diameter"	0.03 to 28	15 to 107	0.3 to 0.6

Least squares techniques were used (2) to determine a dimensionless correlation, except for one dimensional term, for predicting Int_3 from the wind tunnel deposition velocity data for the five surfaces, (a total of 180 data points), for nonreentrainment conditions. After the best data fit was obtained (a multiple correlation coefficient of 0.93 with all terms statistically significant at the 99% level), some deposition velocity predictions were made. However for particle diameters below about 5×10^{-2} μm, deposition velocity predictions did not increase with decreasing particle diameter. An increase should be caused by increased Brownian diffusion rates for smaller particles. It became apparent that the relatively few experimental data points in the minimum deposition velocity range were not being sufficiently weighted (all points were equally weighted) in the data fit. Constants for this best fit model were subsequently redetermined by a weighted least squares technique. The weight was the natural logarithm of the reciprocal of particle diameter in cm. Thus the weight of a 0.03 μm diameter particle was 2.2 times the weight of a 30 μm diameter particle.

The unweighted correlation (2) for the integral mass transfer resistance, Int, is

$$\begin{aligned} Int_3 = - \exp\Big\{ & - 408.728 \\ & + \left[\ln Sc\right]\Big[17.858 - 0.0363 \ln \left(\frac{d}{z_o}\right) \\ & + \left[\ln \tau^+\right]\Big[-14.336 - 0.3441 \ln \tau^+ \\ & + 0.3744 \ln\left(\frac{d}{z_o}\right) - 0.4103 \ln\left(\frac{D}{z_o\, u_*}\right)\Big] - 12.783 \ln d\Big\} \end{aligned} \tag{12}$$

while the weighted correlation is

$$\begin{aligned} Int_3 = - \exp\Big\{ & - 378.051 + 16.498 \ln(Sc) \\ & + \left[\ln \tau^+\right]\Big[-11.818 - 0.2863 \ln \tau^+ \\ & + 0.3226 \ln\left(\frac{d}{z_o}\right) - 0.3385 \ln\left(\frac{D}{z_o\, u_*}\right)\Big] - 12.804 \ln d\Big\}. \end{aligned} \tag{13}$$

In this last case, the multiple correlation coefficient was 0.92 and the group $(\ln Sc)(\ln \frac{d}{z_o})$ was omitted in order to have all coefficients statistically significant at the 99% level.

In both equations the dimensionless relaxation time, τ^+, is calculated for a particle density of 1.5 g/cm^3. Since experimental observations have not been made for other particle densities, the surface integral resistance Int_3 is assumed independent of particle density and is calculated for a particle density of 1.5 g/cm^3.

Int_2 and Int_1

Resistance integrals Int_2 and Int_1 for heights greater than 1 cm were evaluated using Eq. (5) and Bussinger (8) et al., atmospheric diffusion correlations for stable, neutral and unstable conditions. The assumption was an equality of particle eddy diffusivity and eddy diffusivity of air momentum. Since these correlations do not include any canopy effect on eddy diffusivity in box 2, Int_2 and Int_1 were combined into a single resistance integral. The combined resistance integral was calculated from 1 cm up to 1 m, and added to Int_3 (Eq. 13) in order to predict deposition velocities K_{1-m}, for a 1 m reference concentration height.

Integral Resistance Ranges

Predictions were made for the surface mass transfer resistance integral within 1 cm of the deposition surface, Int_3, and compared with atmospheric diffusional resistances. Atmospheric diffusional resistances were calculated from the integrals in Eq. (5) by assuming Brownian diffusion was zero and an equality between particle and air momentum (6) diffusivity. These atmospheric resistances (4) are shown in Figure 1 as a function of height and stability. Since eddy diffusion is least in stable atmospheres, mass transfer resistance integrals were largest for stable atmospheres. The largest shown is -30. For unstable atmospheres, mass transfer resistance integrals were least. For atmospheric instability, the largest resistance integral is -15.5. By contrast, in magnitude, Int_3 surface resistance integrals ranged from -1 to -10^5. These values indicate that box 3 surface resistance is usually controlling overall mass transfer.

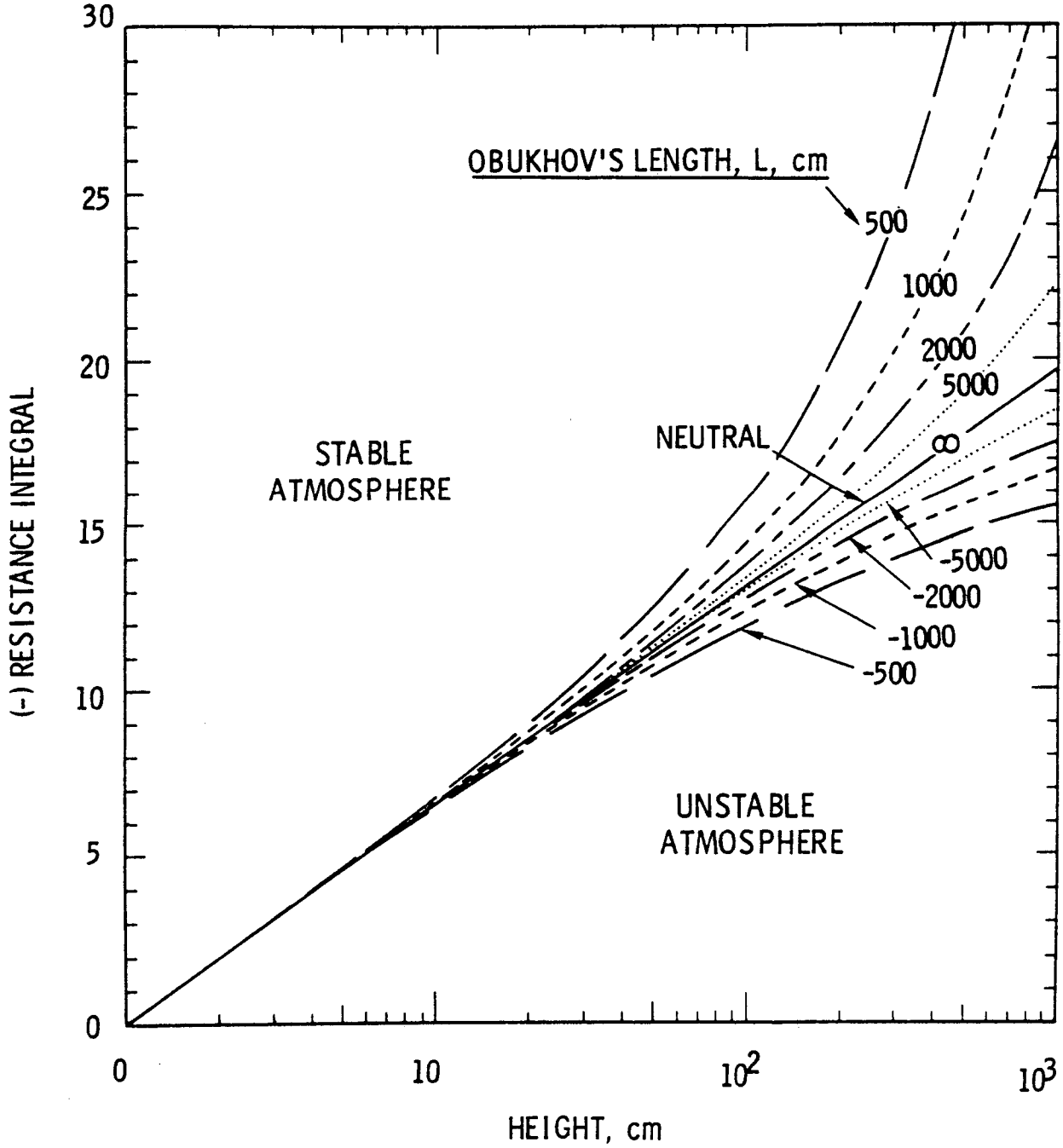

Neg 745530-1

FIGURE 1. Resistance Integral from 1 cm to Indicated Height

Deposition Velocity as a Function of Height

Predicted deposition velocities were calculated from the Int_3 correlation, Eq. (13), and integral resistances above 1 cm to 10 cm, to 1 m, and to 10 m from Figure 1. Predicted deposition velocities shown in Figure 2 were calculated at each height for both unstable and stable atmospheres. The upper bound for each height is for an unstable atmosphere with Obukhov's length equal to -10 m while the lower bound is for a stable atmosphere with Obukhov's length equal to +10 m. The bounds merge into one indistinguishable line for reference heights of 1 and 10 cm. Between particle diameters from about 10^{-1} to 1 μm, all predictions are nearly identical. Consequently in this range, curves are shown only for reference heights of 1 cm and 10 m. All predicted deposition velocities are greater than particle terminal settling velocities indicated by the $K = v_t$ curve for no flow conditions and a particle density of 1.0 g/cm^3. Deposition velocities are a function of particle diameter and have their smallest values in the 0.1 to 1 μm particle diameter range. For larger particles, both increased effective eddy diffusion in Int_3 and increased gravity settling rates tend to increase predicted deposition velocities above the minimum. For smaller particles, deposition velocities increase with decreasing particle diameter because of increased mass transfer by Brownian diffusion.

For reference purposes, deposition velocities with a 1 cm reference concentration height are shown as an upper curve. As expected from increased mass transfer resistance, deposition velocities for larger reference concentration heights are always less than for a 1 cm reference concentration height. However, deposition velocities are almost insensitive to changes in reference concentration at elevated heights of 10 cm, 1 m, and 10 m. This sensitivity appears less pronounced at 1 m and above. Due to this insensitivity, a 1 m reference height was selected for presentation in most deposition velocity figures. We must remember that even with a relative insensitivity to height at 1 m, deposition velocities are only an approximation to describe the unsteady state diffusion-transport boundary limits. It is fortunate that deposition velocities are relatively insensitive to height at 1 m since field experiments and predictions have often used a similar height.

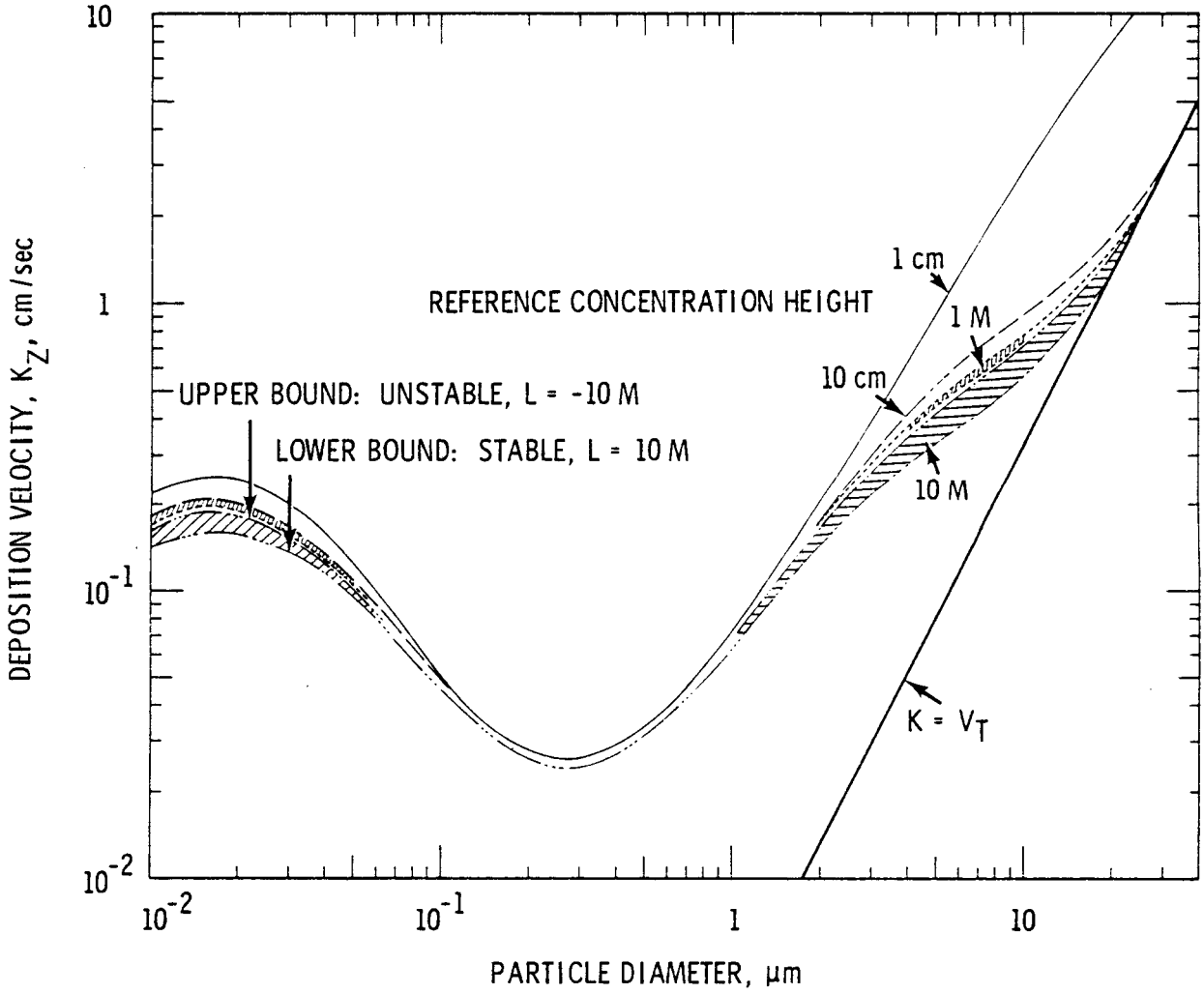

Neg 7712645-1

FIGURE 2. Model-1977W - Predicted Deposition Velocities at Indicated Height for U_* = 20.0 cm/sec, Z_0 = 3.0 cm and Particle Density = 1.0 g/cm^3

Deposition velocities, K_{1-m}, are a function of particle diameter from 10^{-2} to 100 μm. Minimum deposition velocities occur for particle diameters from about 0.2 to 0.3 μm. For smaller particles, deposition velocities increase because of increased mass transfer caused by Brownian diffusion. For larger particles, deposition velocities increase because of increased mass transfer caused by eddy diffusion and gravity settling. In all cases, predicted deposition velocities are greater than predicted by simple gravity settling, v_t. These deposition velocities are for a particle density of one g/cm^3 and a constant roughness height of 3 cm. This is a typical height for the Hanford Reservation.

One might propose that atmospheric stability might have a major influence on particle deposition. However, two predicted deposition velocities curves at each height show a minor influence of atmospheric stability on deposition. The upper curve is for an unstable atmosphere with an Obukhov's length of -10 m and the lower curve is for a stable atmosphere with an Obukhov's length of 10 m.

Controlling Mass Transfer Resistances

Relative resistances or controlling resistances can sometimes become more apparent from the changes in deposition velocity with reference concentration height. Consequently, deposition velocities were calculated for Figure 3 in which some mass transfer resistances were assumed zero. Three regions are shown as a function of height for atmospheric diffusion and gravity settling between 10 cm to 1 cm, 1 m to 1 cm, and 10 m to 1 cm and no resistance below 1 cm. For the 10 m region, both the upper unstable atmosphere bound and the lower stable atmosphere bound are shown as well as a neutral stability curve, ($\varepsilon = ku_*z$), between these bounds. For particle diameters smaller than about 3 μm, deposition velocities range from 0.4 to 1 cm/sec. In contrast when resistance is included below 1 cm, deposition velocities calculated for a 1 cm reference height are considerably smaller. Thus, we may conclude the surface mass transfer resistance in the lower 1 cm controls the overall deposition. This control was shown in Figure 2 in

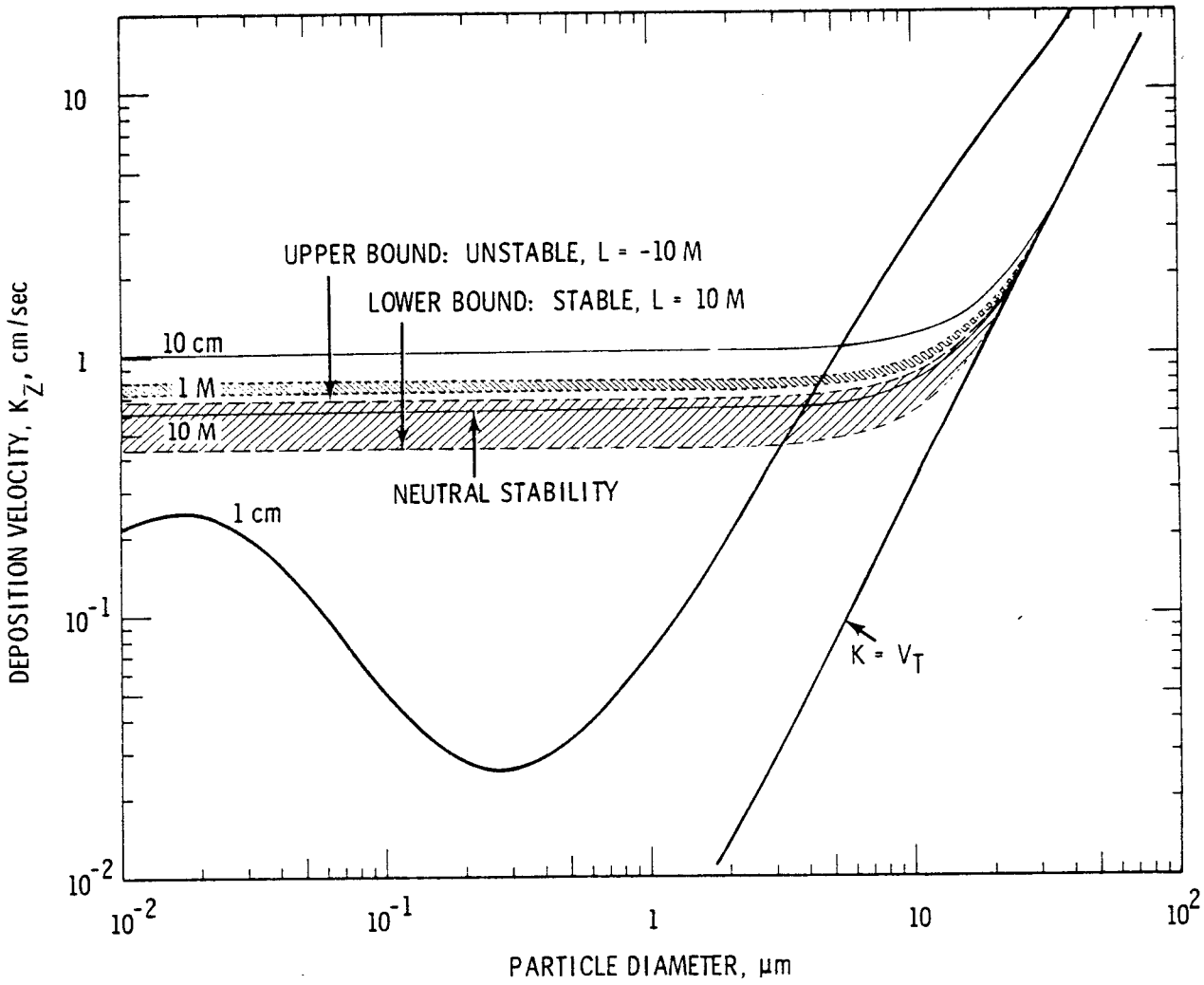

Neg 7712645-2

FIGURE 3. Model-1977W - Predicted Deposition Velocities at Indicated Height for U_* = 20 cm/sec, Z_o = 3.0 cm with no Surface Resistance (INT_3=0) Below 1 cm and Particle Density = 1.0 g/cm^3

which the deposition velocity was relatively insensitive to reference concentration heights from 1 cm to 10 m for particle diameters smaller than about 3 μm.

The relative resistance above 1 cm as compared to below 1 cm is a function of particle diameter. The resistance above 1 cm becomes increasingly controlling as particle diameters are increased above about 6 μm. For these particle diameters, deposition velocities are larger for a 1 cm reference height than for reference heights from 10 cm to 10 m. Thus, when resistances are analytically summed by use of Eq. (5), predicted deposition velocities at elevated heights are considerably less than for 1 cm. This was shown in Figure 2.

Deposition Velocity as a Function of Friction Velocity

Deposition velocities and relative mass transfer resistances are also a function of friction velocity. Deposition velocities for a 1 m reference height and a 3.0 cm surface roughness are shown in Figure 4 for the case of no surface resistance below 1 cm. Deposition velocities increase as friction velocity is increased from 10 to 200 cm/sec. These deposition velocities are large and again suggest a small relative mass transfer resistance between 1 cm to 1 m.

When the mass transfer resistance below 1 cm is combined with that between 1 cm and 1 m, deposition velocities are significantly reduced below those shown in Figure 4. These K_{1-m} deposition velocities are shown in Figure 5 for a neutral atmosphere. This figure again shows minimum deposition velocities for a particle diameter of about 0.2 to 0.3 μm. Deposition velocities are a function of friction velocity for a constant aerodynamic surface roughness. For particle diameters outside the range from 0.1 to 1 μm, deposition velocities always increase with an increase in friction velocity. In contrast within the 0.1 to 1 μm diameter range, there is a minimum deposition velocity of 0.025 cm/sec which occurs for a friction velocity in the range of 20 to 30 cm/sec. It is unknown whether this minimum is physically real or only reflects uncertainties in the Int

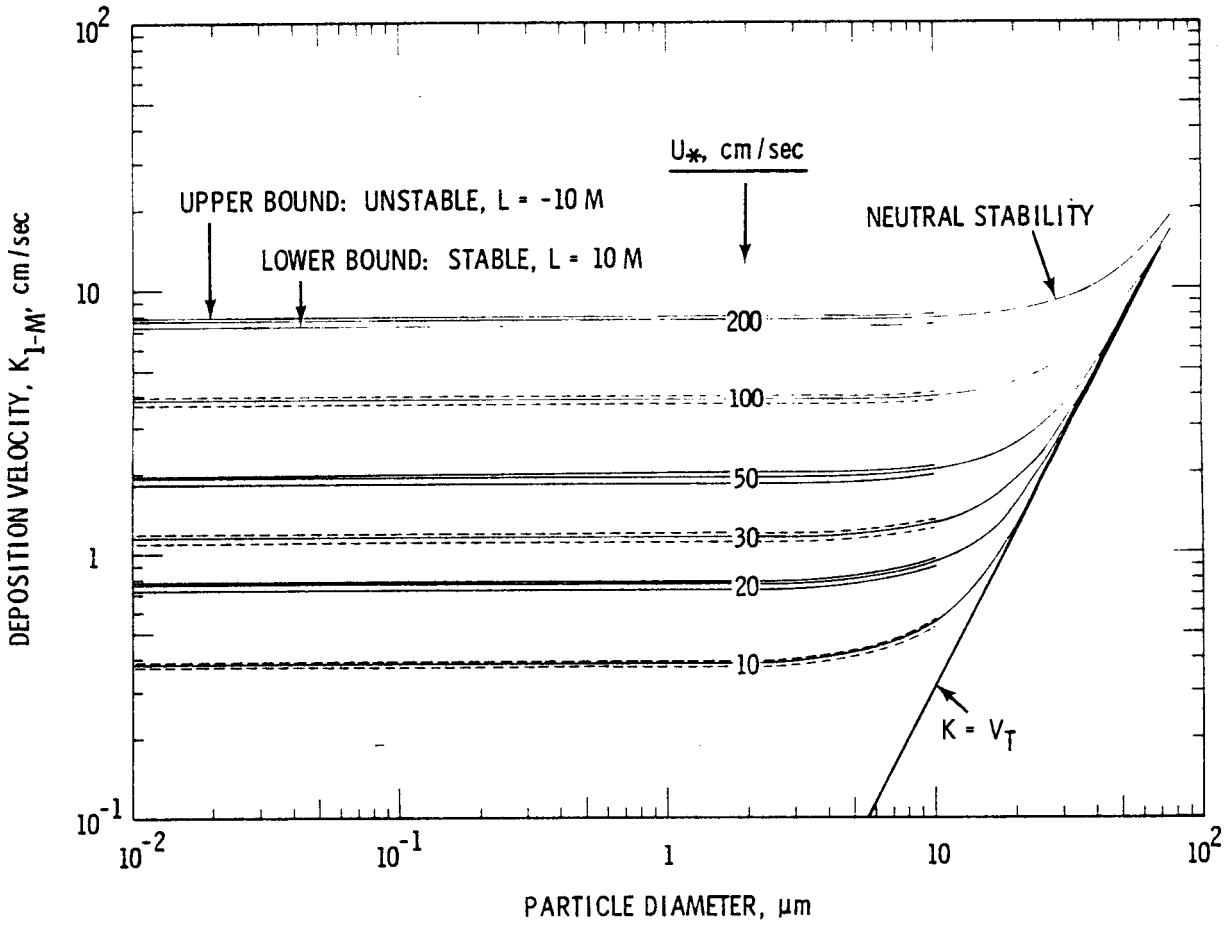

Neg 7712645-4

FIGURE 4. Model-1977W - Predicted Deposition Velocities at 1M Height for Z_o = 3.0 cm with no Ground Resistance (INT_3=0) Below 1 cm and Particle Density = 1.0 g/cm^3.

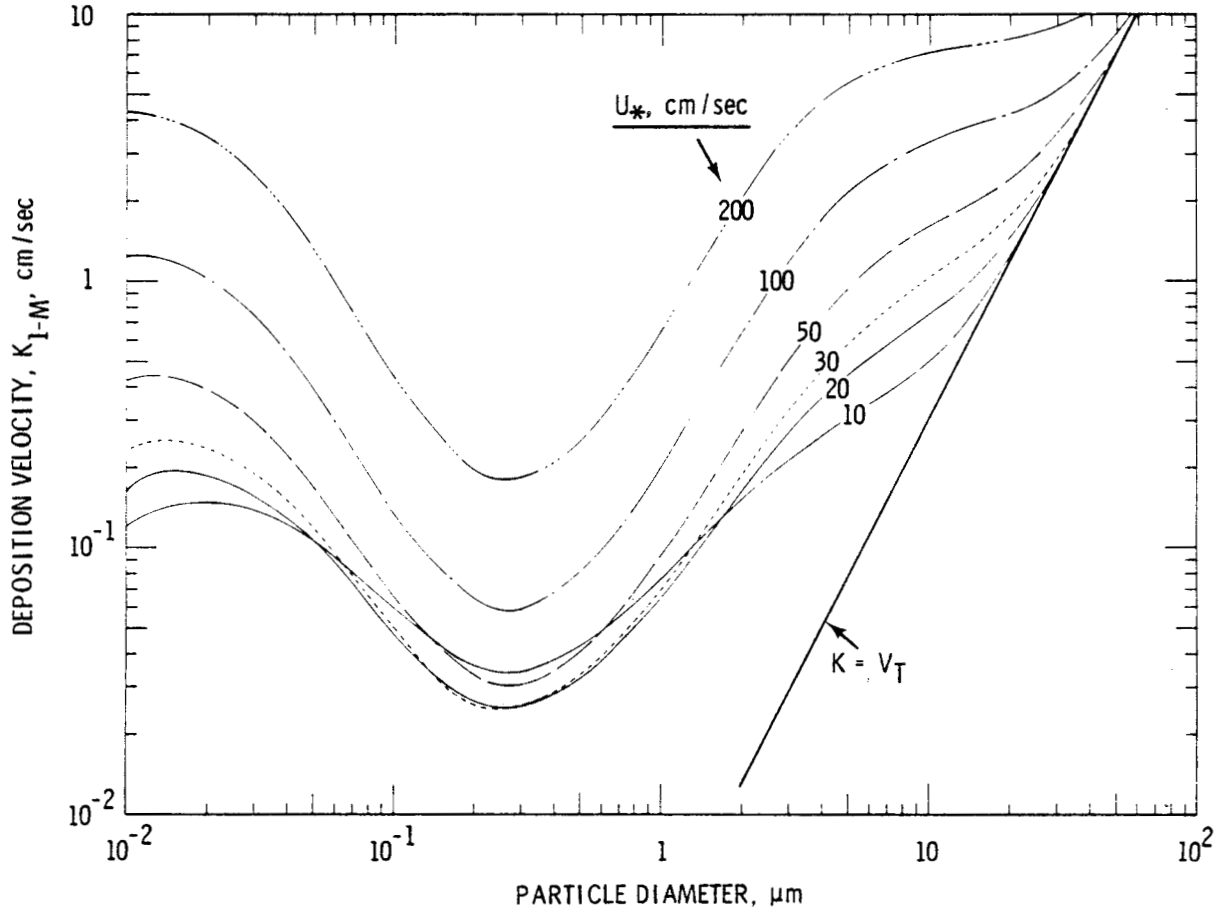

Neg 7712645-3

FIGURE 5. Model-1977W - Predicted Deposition Velocities at 1M Height for Z_0 = 3.0 cm and Neutral $\varepsilon = kU_*Z$

correlation given in Eq. (13). By cross comparing curves from Figures 6 to 12, the 20 to 30 cm/sec friction velocity range predicts the minimum deposition velocity for all aerodynamic surface roughnesses from 10^{-3} to 10 cm.

Deposition Velocities at 1 m

Deposition velocities, K_{1-m}, were predicted (2) as a function of particle diameter from 10^{-2} to 100 μm, friction velocities, u_*, from 10 to 200 cm/sec, roughness height, z_0, from 10^{-3} to 10 cm, particle density from 1 to 11.5 g/cm^3 and atmospheric stabilities for Obukhov's lengths from -10 to +10 m (unstable and stable atmosphere, respectively). These predictions indicate deposition velocities can vary several orders of magnitude from about 10^{-3} to 10 cm/sec and increase with an increase in roughness height z_0 and usually with an increase in friction velocity u_*.

Predicted deposition velocities, K_{1-m}, for a stable atmosphere are shown in Figure 5 for a 1 m concentration reference height and a constant friction velocity of 30 cm/sec. For particle diameters below about 10^{-2} μm, Eq. (13) predicts too large a surface resistance. Consequently, a lower limit curve was calculated. For the calculation, the Int_3 term was replaced by

$$Int_s = -\int_{z^+ \text{ at } 1 \text{ cm}}^{a^+ = 0} \frac{dz^+}{D/\nu} \tag{14}$$

to account for mass transfer only by Brownian diffusion next to the deposition surface and diffusion for a stable atmosphere from the indicated height to 1 m. In this case, deposition velocities increase with a decrease in particle diameter. Also shown is a curve for only Brownian diffusion in the lower 0.1 cm. With this diffusional distance decrease from 1 cm to 0.1 cm, these lower limits for deposition velocities increased nearly two orders of magnitude. Obviously, predicted deposition velocities for these small particles are dependent upon Brownian diffusion adjacent to the deposition surface.

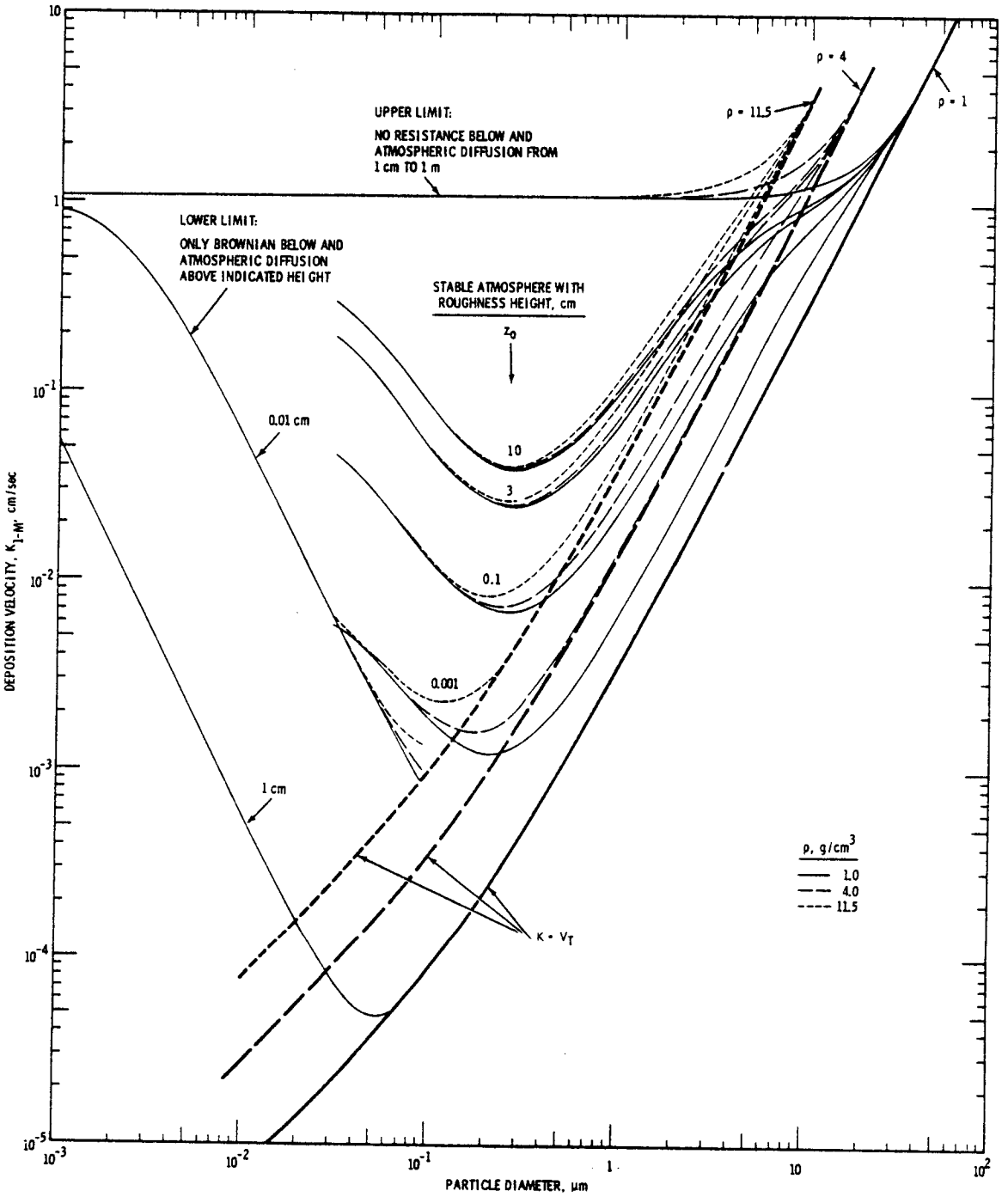

Neg 7711495-2

FIGURE 6. Model-1977W - Predicted Deposition Velocities at 1M for U_* = 30 cm/sec and Particle Densities of 1, 4 and 11.5 g/cm3

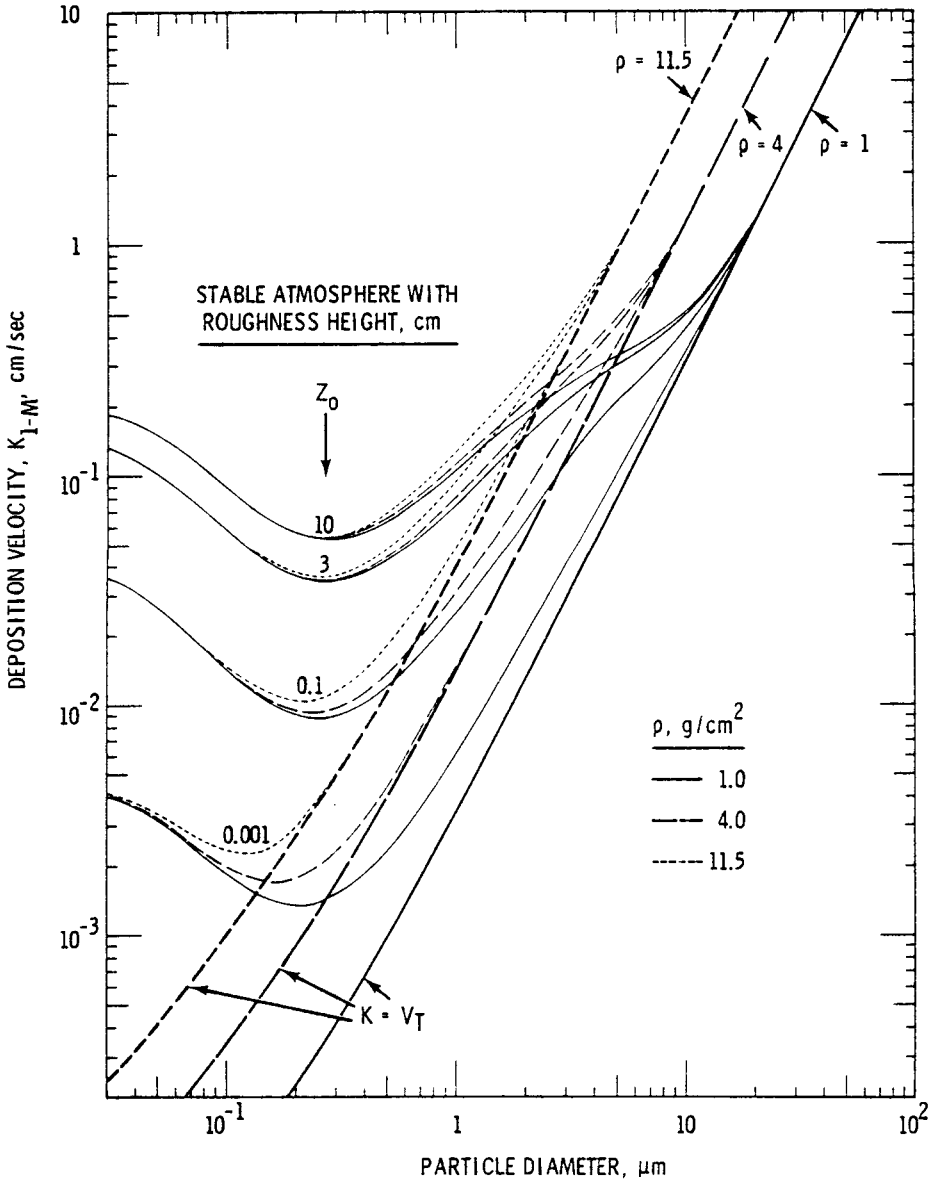

Neg 7712644-1

FIGURE 7. Model-1977W - Predicted Deposition Velocities at 1M for U_* = 10 cm/sec and Particle Densities of 1, 4 and 11.5 g/cm^3

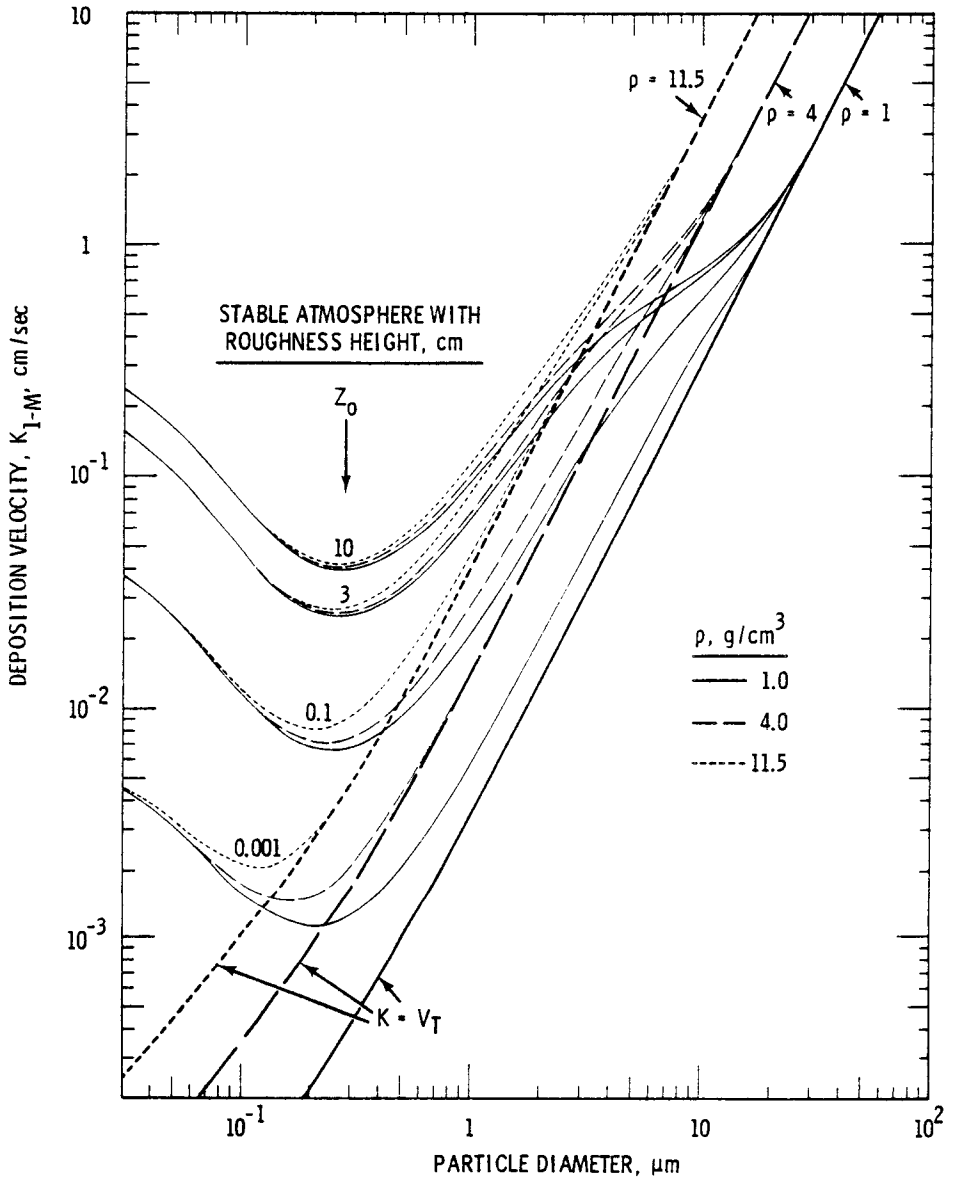

Neg 7712644-2

FIGURE 8. Model-1977W - Predicted Deposition Velocities at 1M for U_* = 20 cm/sec and Particle Densities of 1, 4 and 11.5 g/cm^3.

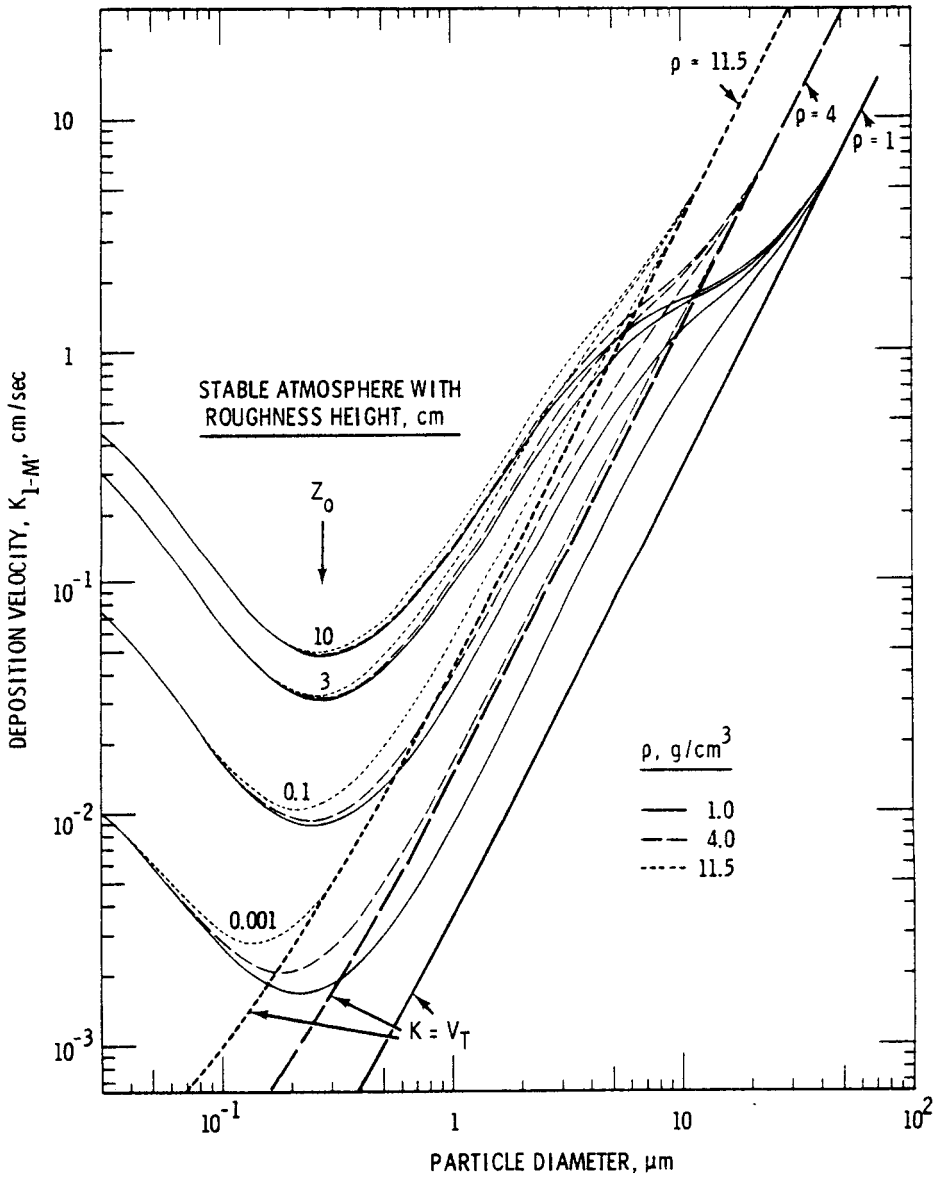

FIGURE 9. Model-1977W - Predicted Deposition Velocities at 1M, for U_* = 50 cm/sec and Particle Densities of 1, 4 and 11.5 g/cm^3

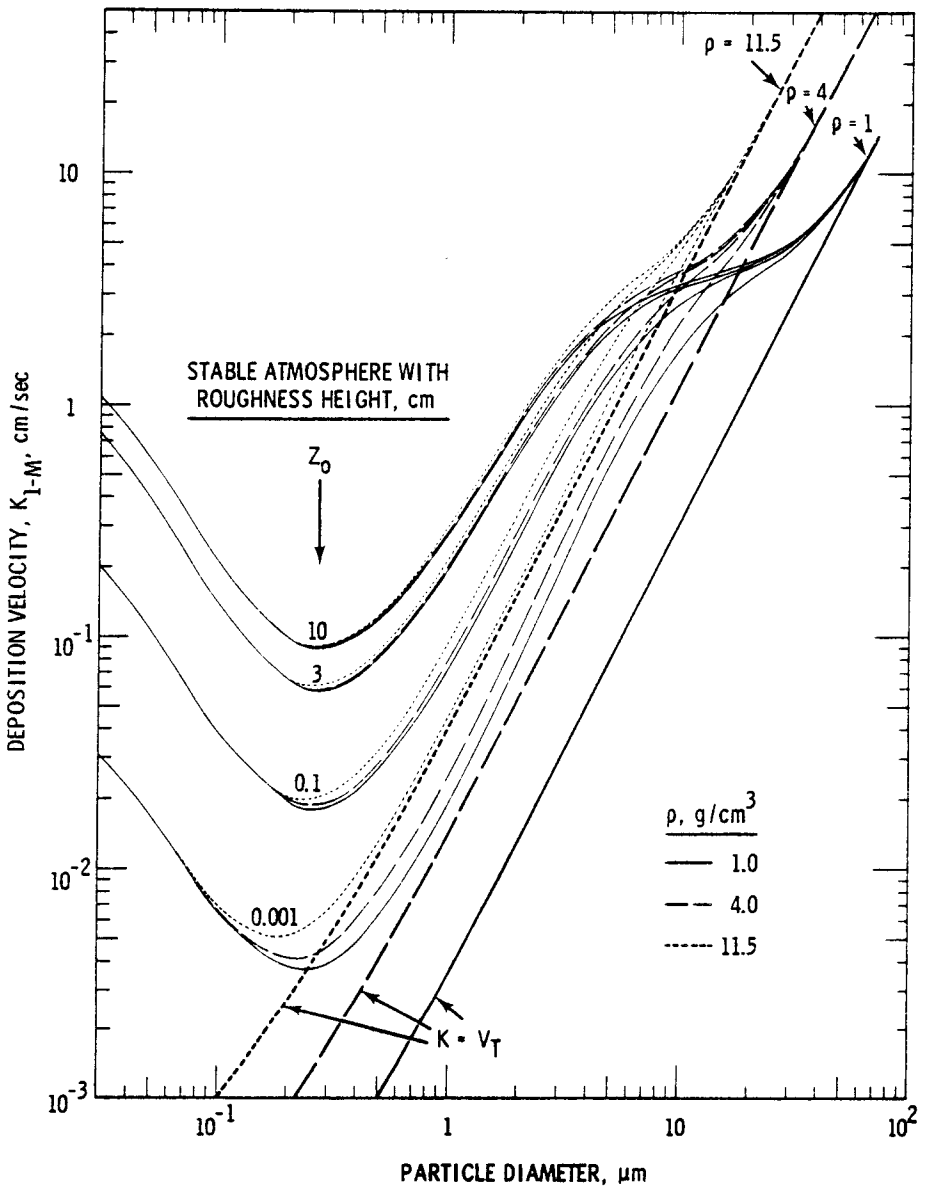

Neg 7712644-4

FIGURE 10. Model-1977W - Predicted Deposition Velocities at 1M for U_* = 100 cm/sec and Particle Densities of 1, 4 and 11.5 g/cm^3

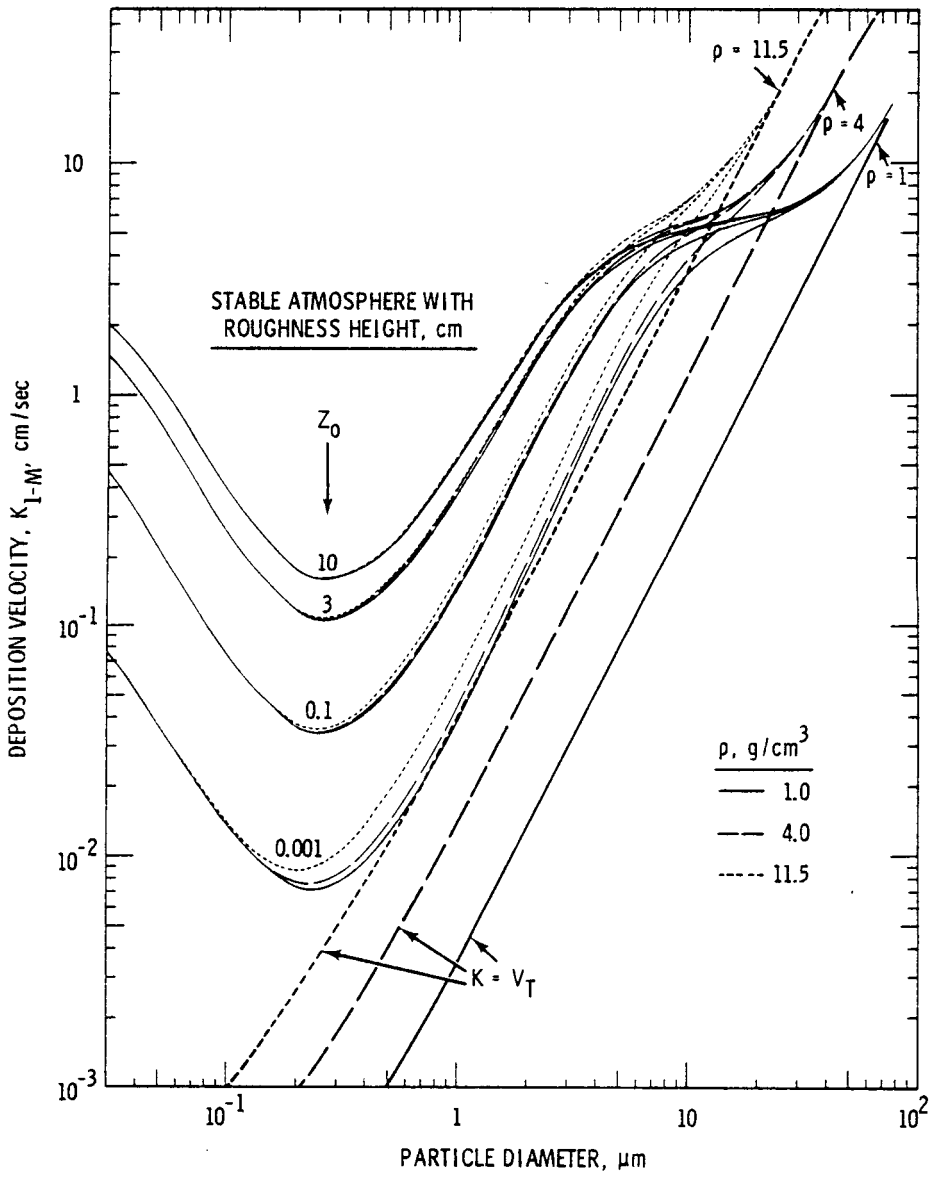

Neg 7712644-5

FIGURE 11. Model-1977W - Predicted Deposition Velocities at 1M for U_* = 150 cm/sec and Particle Densities of 1, 4 and 11.5 g/cm^3

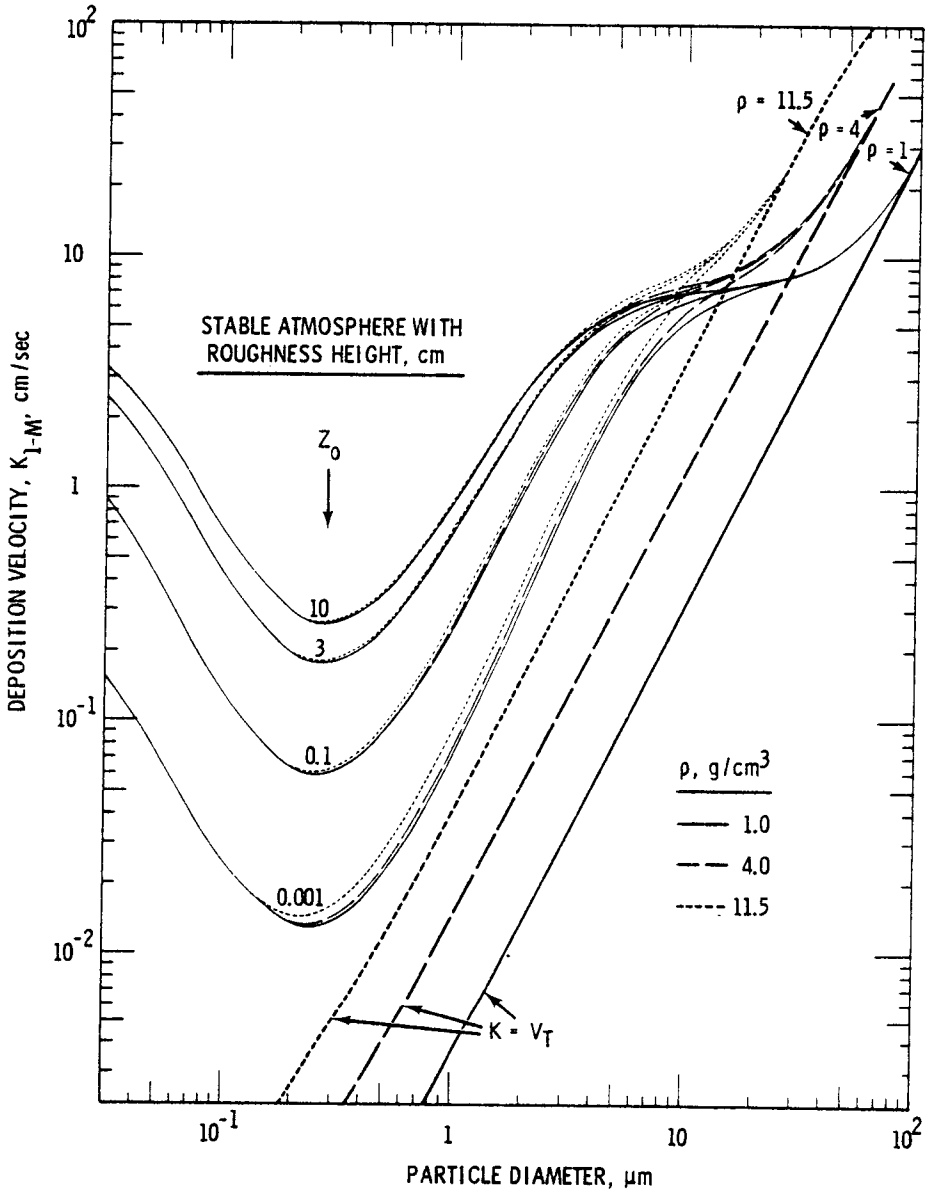

Neg 7712644-6

FIGURE 12. Model-1977W - Predicted Deposition Velocities at 1M for U_* = 200 cm/sec and Particle Densities of 1, 4 and 11.5 g cm^3

An upper limit to dry deposition velocities was also calculated. In this case, the Int_3 term on the right side of Eq. (5) was assumed to be zero. Deposition velocities were calculated by assuming atmospheric diffusion and the particle terminal settling velocity control deposition between 1 cm and 1 m. For particle diameters below 1 μm, the upper limit is nearly constant and decreases from 1.1 cm/sec at 1 μm to 1.08 cm/sec at 10^{-3} μm. For field data in comparison, deposition velocities are reported greater than 1 cm/sec for some gases. Thus, this upper limit is an approximation which is limited by uncertainties in the available surface area for deposition and in the particle eddy diffusivity. As a calculation simplification, only the ground surface area is used rather than the total canopy surface area. Similarly, the eddy diffusivity of momentum rather than heat (heat would have a factor of up to 1.3 higher) was used for the particle eddy diffusivity. If heat diffusivity had been used, the predicted upper limit might be 1.3 greater for a reasonably smooth field. However, most surfaces are not smooth. Thus, in general, the canopy effects on any diffusivity can not be adequately predicted. For the diffusivity assumed, deposition velocities increase for particle diameters above about 2 μm. For even larger particle diameters, deposition velocities increase and approach the respective terminal settling velocities for each particle density.

Deposition velocities are shown for a constant friction velocity of 30 cm/sec in Figure 6. Curves are shown for particle densities of 1, 4, and 11.4 g/cm^3 and roughness heights of 10^{-3}, 10^{-1}, 3, and 10 cm. In all cases, predicted deposition velocities are greater than the particle terminal settling velocity.

Deposition velocities increase with an increase in both surface roughness and particle density. However, deposition velocities are independent of particle density for small particles where Brownian diffusion controls mass transfer. Brownian diffusion is controlling in the particle size region in which the three density curves merge for particle diameters less than about 0.1 μm.

CANOPY LIMITATION

Dry deposition velocity for predictions can be calculated from the model for most variables except available deposition surface area. Prediction procedures cannot yet describe the effects of foliage density on deposition velocities, nor particle penetration through the foliage to the underlying surface. Consequently, penetration results and foliar deposition velocities are needed to improve deposition velocity models.

Large particle penetration results were determined in a wind tunnel (10) for a crushed gravel (3.8 to 5.8 cm diameter) surface and also penetration and deposition velocities for an artificial tree foliage fetch 9 cm high. The artificial tree foliage fetch was 23 cm by 30 cm. Trees were mounted in a rectangular array with eight downwind rows of six trees. Tree spacing was 3.8 cm. The polyethylene trees were 7 to 9 cm high with a maximum crown width of 4 to 6 cm. Each crown had eight branches located around the central trunk, and the tree trunk extended $\sim$2 cm below the crown.

Nonuniform particle deposition in the tree fetch indicated edge effects. Depending upon particle diameter and wind speed, the front row of trees usually had either more or less deposition than downwind rows. These edge effects extended for three to five rows. Since particle penetration to the entire plate was significant, deposition velocities for each row could not be calculated. Thus, average deposition velocities for all trees and the plate are shown in Figure 13. The two wind speeds were measured upwind and at a 6 cm height which is approximately the height of the tree crown mid-plane.

Deposition velocity curves show different patterns than those for the simpler surfaces predicted in Figures 13 through 15. At a wind speed of 2 m/sec approaching the trees, a minimum deposition velocity occurs at about 1 to 2 μm for the trees. In contrast, simpler surfaces exhibit minima in the particle diameter range from 0.1 to 1 μm. For a 13 m/sec wind speed approaching the trees, deposition velocities are nearly constant for all particle diameters studied. Again, in contrast, deposition velocities for 2 μm compared to larger particles would be significantly less for simpler surfaces.

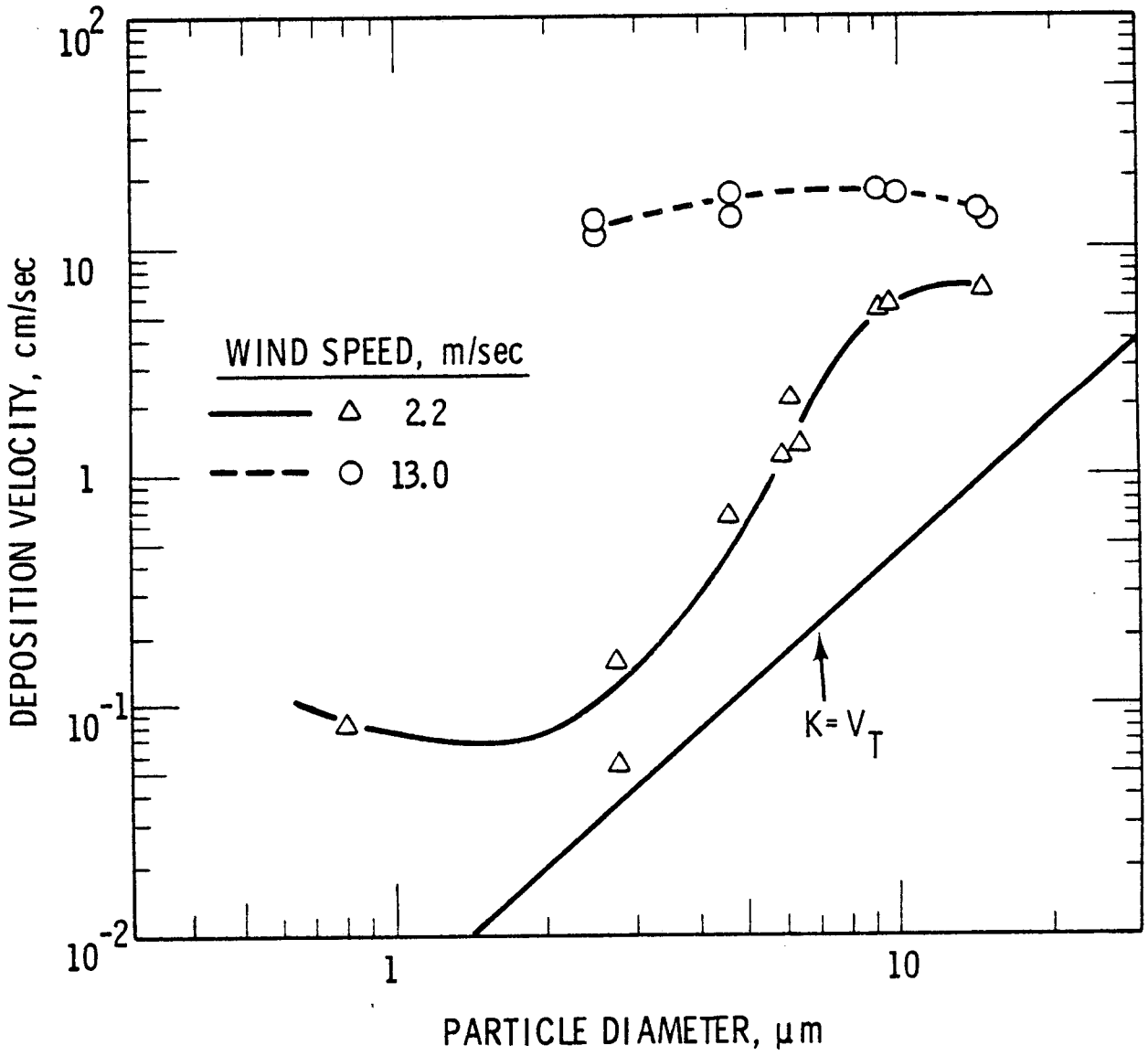

Neg 760188-3

FIGURE 13. Deposition Velocities to a Canopy of Plastic Trees 9 cm High

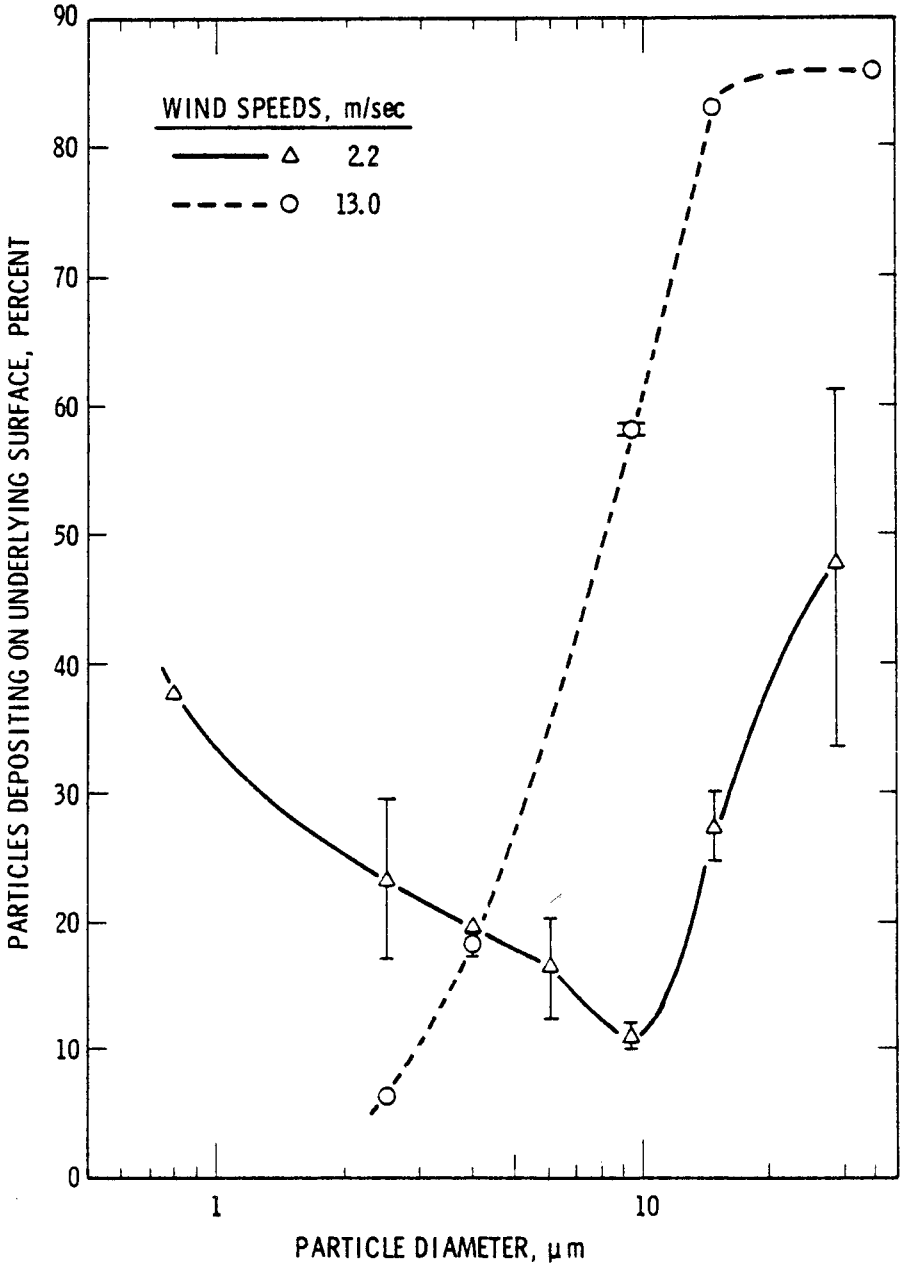

Neg 760188-1

FIGURE 14. Penetration of Depositing Particles Through a Canopy of Plastic Trees (Trees 9 cm High and 3.8 cm Wide, in 8 Downwind Rows of 6 Trees Each)

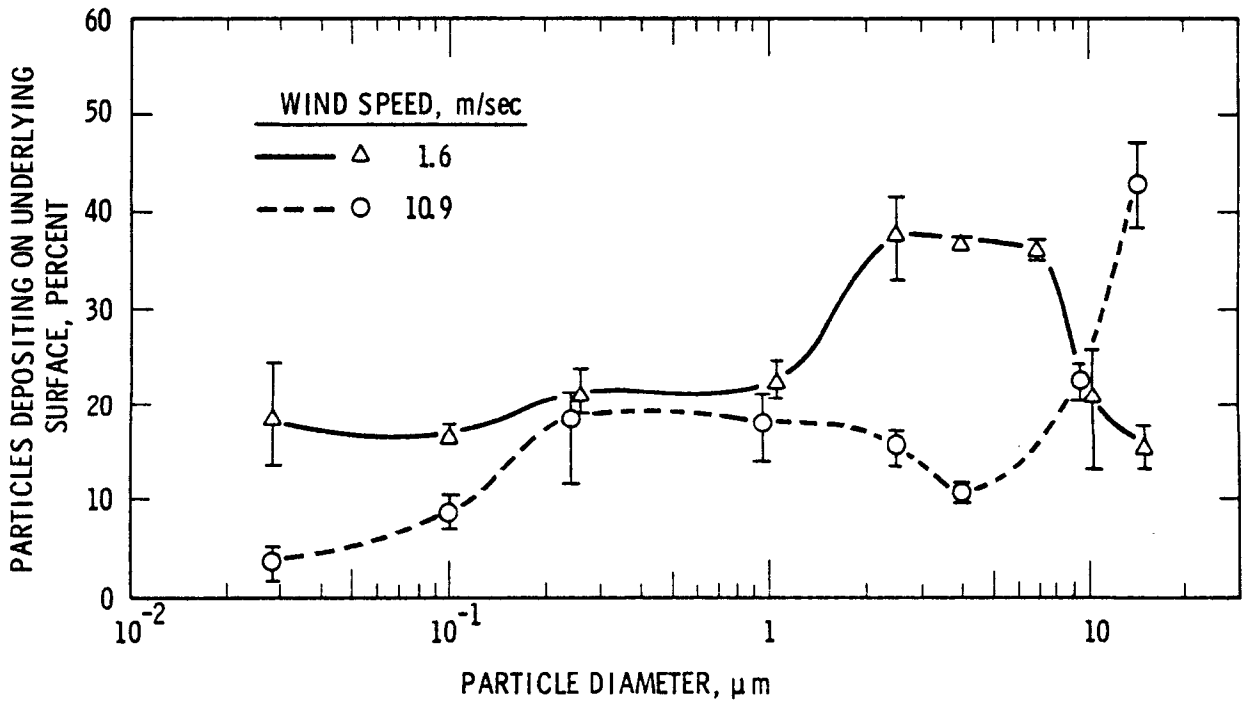

Neg 760188-2

FIGURE 15. Penetration of Depositing Particles Through 3.8 to 5.1 cm Diameter Crushed Rock to an Underlying Surface

Particle penetration to the plastic mounting base for the trees is shown in Figure 14. Penetration is the deposition to the plate as a percent of the deposition to the plate and trees. Maximum penetration was 83%. Penetration is a complex function of both wind speed and particle diameter. For particles smaller than 4 μm diameter, penetration is greatest at the low wind speed. For larger particles than this 4 μm diameter cross-over, penetration is greatest at the high wind speed.

As shown in Figure 15, a cross-over diameter was also shown for penetration through crushed gravel. At the slower (1.6 m/sec) wind speed, penetration is greater for particle diameters from 3×10^{-2} μm up to the 9 μm cross-over diameter. The two wind speeds were measured 3 cm above the gravel surface.

The penetration curves for crushed gravel and trees are similar. Penetration is larger for the slow wind speeds for particle diameters below the cross-over point. However, the particle diameter at the cross-over point is a factor of two (4 versus 9 μm) less for trees than for crushed gravel. Apparently the nonrigid tree motion and open tree structure tend to enhance resuspension at the smaller 4 μm particle diameter as compared to 9 μm for the rigid and more dense gravel structure. For particles larger than the cross-over point, penetration was always greater at the higher wind speed.

An explanation was sought for these penetration similarities. One possibility is that above the cross-over point deposition and resuspension occurred simultaneously at the higher wind speed. It can be conjectured that particles resuspended from the upper surfaces of the gravel and trees while the flux of penetrating particles remained constant. In this case, the observed penetration would increase since fewer particles remained deposited on the upper surfaces. For particles smaller than the cross-over diameter, a satisfactory suggestion is yet needed to explain higher penetration at lower wind speeds. Possibly, for these particle relaxation times, the air turbulence scale and intensity or relative wind profiles through the canopies are sufficiently different for the two wind speeds.

CONCLUSIONS

Predictive deposition velocity models must eventually consider both deposition within vegetative canopies as well as deposition penetration to the underlying surface. However, this penetration data base is very limited and consequently penetration cannot yet be generalized in predictive models. Deposition velocities to vegetation (9 cm trees) do show edge effects at the entrance to the "grove" of vegetation. Similar edge effects may be very important within forests since most forests contain many clearings from small to large size. Indications are that resuspension could probably occur simultaneously with deposition on the upper surfaces of vegetation.

Deposition velocities have been determined for field conditions, but data have never been organized into a unified approach for extending predictions to other test conditions. In contrast, this paper develops a predictive method for field conditions for a particle density of 1.5 g/cm^3. For other particle densities, the integral resistance, Int_3, was assumed independent of particle density. There are problem areas in applying these deposition velocities. Deposition velocities are a function of particle diameter even when all other variables are constant. Thus in either applying or interpreting deposition velocities to field conditions, one must adequately describe the particle size distribution.

Deposition velocities are nearly independent of particle diameter only in the 0.1 to 1 μm size range. Since deposition velocities increase rapidly above 1 μm, even a few percent of particles being greater than 1 μm in diameter can significantly alter the average deposition velocity.

Use of a three box mass transfer model and the dimensionless resistance integral requires that sufficient experimental data should always be recorded when experimentally evaluating deposition velocities. Required data include at least friction velocity, roughness height, particle size distributions, and atmospheric stability. In addition, airborne concentration should be measured at several heights in order to determine the airborne concentration, as a function of height. If this profile is known,

one can determine if the airborne concentration is nearly insensitive to height at the height selected for defining the deposition velocity (Eq. 2). If the airborne concentration is dependent on height, a better approximation than a single deposition velocity must be developed to include the atmospheric delivery capability. Concentration data will be required if more realistic deposition velocity predictions or correlations are ever to be made with multi-box mass transfer models.

ACKNOWLEDGMENT

This paper is based on work performed under U.S. Department of Energy Contract EY-76-C-06-1830.

NOMENCLATURE

a = particle radius, cm

C = airborne concentration of monodispersed particles, cm^{-3}

d = particle diameter, cm

D = Brownian diffusion coefficient cm^2/sec, (see Equation 15)

Int = Integral mass transfer resistance next to surface, dimensionless

k = Boltzmann's constant, 1.32×10^{-16} erg/(molecule °K)

p = pressure, cm of mercury (76.0 cm used)

Sc = Schmidt number, ν/D

T = temperature, °K (296°K used)

u_* = friction velocity, cm/sec

v_t = monodispersed particle gravity settling velocity, cm/sec

z_o = aerodynamic surface roughness, cm

z^+ = dimensionless height, zu_*/ν

μ = air viscosity, g/(cm·sec), [1.78×10^{-4} g/(cm·sec) used]

ν = kinematic viscosity, μ/ρ

ρ = air density, g/cm^3, (1.2×10^{-3} g/cm^3 used)

ρ_p = particle density, g/cm^3 (1.5 g/cm^3 used)

τ^+ = dimensionless relaxation time, $\frac{\rho_p d^2}{18\,\mu} \frac{u_*^2}{\nu}$

The Brownian diffusivity was calculated (11) from

$$D = \frac{kT}{6\pi\mu a} \left\{1 + \frac{10^{-4}}{pa} [6.32 + 2.01 \exp(-2190pa)]\right\} \qquad (15)$$

APPENDIX

Roughness Height and Friction Velocity

Deposition velocities are a function of the aerodynamic surface roughness, z_0, and friction velocity, u_*. These two values are usually calculated empirically from the air velocity profile above a relatively smooth ground surface by using the expression

$$u = \frac{u_*}{k} \ln \frac{z + z_0}{z_0} , \tag{16}$$

where u is the measured velocity, z is the measured height above ground and k is von Kármán's constant (8) of 0.35. For a surface of greater geometric roughness, the height is adjusted to a zero-displacement plane, d, within the canopy. In this case, the relationship is

$$u = \frac{u_*}{k} \ln \frac{z - d}{z_0} . \tag{17}$$

In using these equations, the quantities d and z_0 are adjusted until straight lines are obtained on semi-log paper. Thus, these d and z_0 values have no physical meaning other than an empirical data fit. Often d is about three-fourths of the canopy height while z_0 might range from 10^{-4} to 10^2 cm (flat plate with d = 0 to a forest with d = 7 m, respectively). Similarly as a rule of thumb, the friction velocity might be a few percent of the average air velocity.

The friction velocity, u_*, was used to nondimensionalize distance in Eq. (4) and is also used in a definition of the eddy diffusivity of momentum. In the case, the friction velocity is defined as

$$u_* = \sqrt{\tau_0/\rho} = \sqrt{\overline{u'v'}} . \tag{18}$$

Now, the turbulent shear stress is

$$\tau_0/\rho = -\varepsilon_M \frac{du}{dz}, \tag{19}$$

or upon combining Eq. (18) and (19) the eddy diffusivity is

$$\varepsilon_M = \frac{\overline{u'v'}}{\frac{du}{dz}} . \tag{20}$$

This diffusivity will be defined in terms of u_*. After differentiation of Eq. (16),

$$\frac{du}{dz} = \frac{u_*}{k(z + z_0)} . \tag{21}$$

Consequently, Eq. (18) and (21) are substituted into Eq. (20) to obtain an expression for the eddy diffusivity of momentum in a neutral atmosphere:

$$\varepsilon_M = k\ u_*(z + z_0) . \tag{22}$$

REFERENCES

1. Van der Hoven, I., "Deposition of Particles and Gases." Meteorology and Atomic Energy. 5-3:202-208, D. H. Slade, ed., (1968).

2. Sehmel, G. A. and W. H. Hodgson, "Improved Predictive Dry Deposition Correlation." Pacific Northwest Laboratory Annual Report for 1977: Atmospheric Sciences, PNL-2500-3, Battelle, Pacific Northwest Laboratories, Richland, WA, in press.

3. Sehmel, G. A. and W. H. Hodgson, "Improved Particle Deposition Model." Pacific Northwest Laboratory Annual Report for 1976 to the ERDA Assistant Administrator For Environmental Safety, BNWL-2100, Part 3, Battelle, Pacific Northwest Laboratories, Richland, WA, 61-65 (1977).

4. Sehmel, G. A. and W. H. Hodgson, "Predicted Dry Deposition Velocities." Proc. of the Atmosphere-Surface Exchange of Particulate and Gaseous Pollutants - 1975 Symposium, Energy Research and Development Administration Symposium Series CONF-740921, National Technical Information Service, U.S. Department of Commerce, 399-422, Richland, WA (September 4-6, 1974).

5. Sehmel, G. A., "Comparison of Deposition Velocities Predicted from Dimensionless Analysis Correlation." Pacific Northwest Laboratory Annual Report for 1975 to the USAEC Division of Biomedical and Environmental Research, Atmospheric Sciences, BNWL-1950, Part 3, Battelle, Pacific Northwest Laboratories, Richland, WA, 175-180 (1975).

6. Sehmel, G. A. and W. H. Hodgson, "Particle Dry Deposition Velocities." Pacific Northwest Laboratory Annual Report for 1974 to the USAEC Division of Biomedical and Environmental Research, Atmospheric Sciences, BNWL-1950, Part 3, Battelle, Pacific Northwest Laboratories, Richland, WA, 175-180 (1975).

7. Sehmel, G. A. and W. H. Hodgson, "Particle and Gaseous Removal in the Atmosphere by Dry Deposition." Symposium on Atmospheric Diffusion and Air Pollution preprint volume, Santa Barbara, CA, September 9-13, 1974, 253-260, American Meteorological Society, Boston, MA (1974).

8. Businger, J. A., J. C. Wyngaard, Y. Izumi and E. F. Bradley, "Flux-profile Relationships in the Atmospheric Surface Layer. "J. Atmos. Sci. 28:181-189 (1971).

9. Sehmel, G. A., W. H. Hodgson, and S. L. Sutter, "Dry Deposition of Particles." Pacific Northwest Laboratory Annual Report for 1973 to the USAEC Division of Biomedical and Environmental Research, Atmospheric Sciences, BNWL-1850-3, Battelle, Pacific Northwest Laboratories, Richland, WA, 157-162 (1974).

10. Sehmel, G. A. and W. H. Hodgson, "Particle Deposition and Penetration Through Vegetation Canopies from Wind Tunnel Experiments." Pacific Northwest Laboratory Annual Report for 1975: Atmospheric Sciences, BNWL-2000-3, Battelle, Pacific Northwest Laboratories, Richland, WA, 86-89 (1976).

11. Davies, C. N., Aerosol Science. Academic Press, NY, 408 (1966).